

Phase structure and critical point in heavy-quark QCD at finite temperature

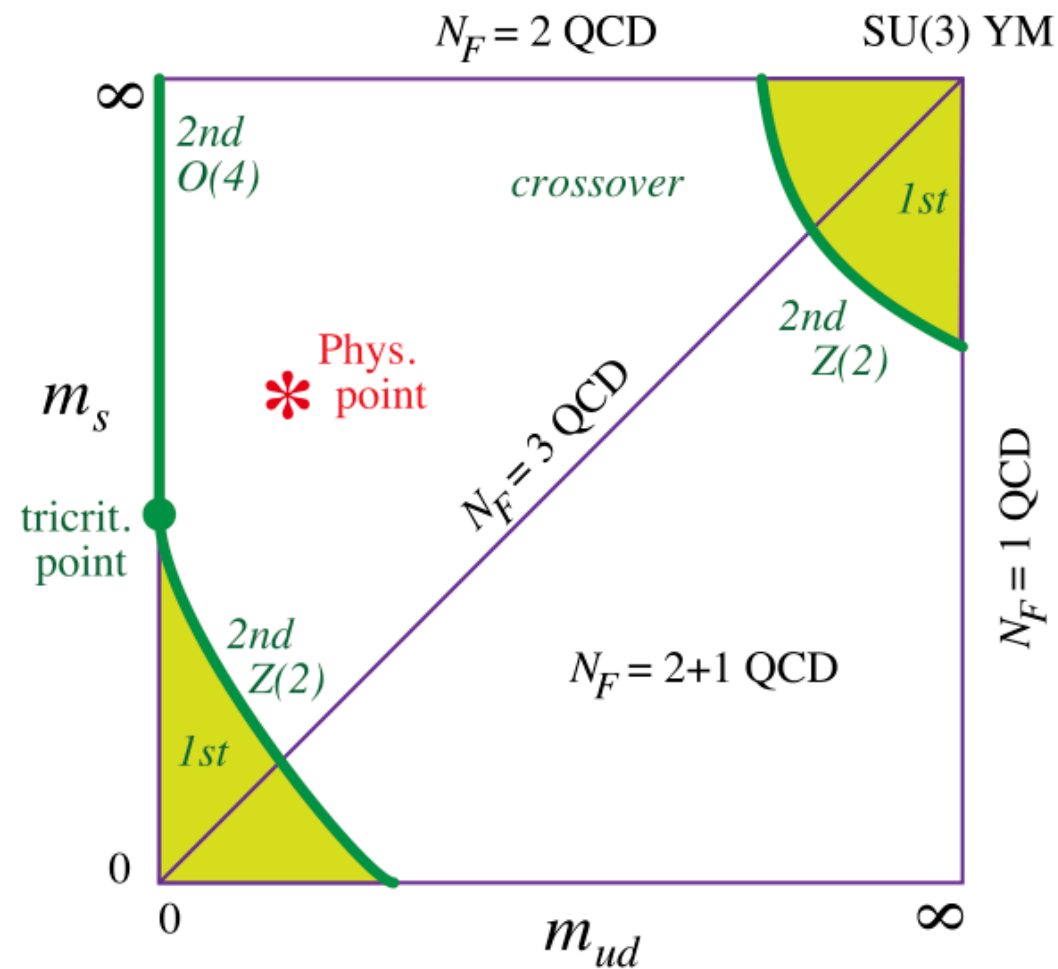
**Kazuyuki Kanaya¹⁾ with Ryo Ashikawa²⁾, Shinji Ejiri³⁾,
Masakiyo Kitazawa^{2,4)}, Hiroshi Suzuki⁵⁾, Naoki Wakabayashi³⁾
(WHOT-QCD Collaboration)**

1) Univ. Tsukuba, 2) Osaka Univ., 3) Niigata Univ., 4) Kyoto Univ., 5) Kyushu Univ.



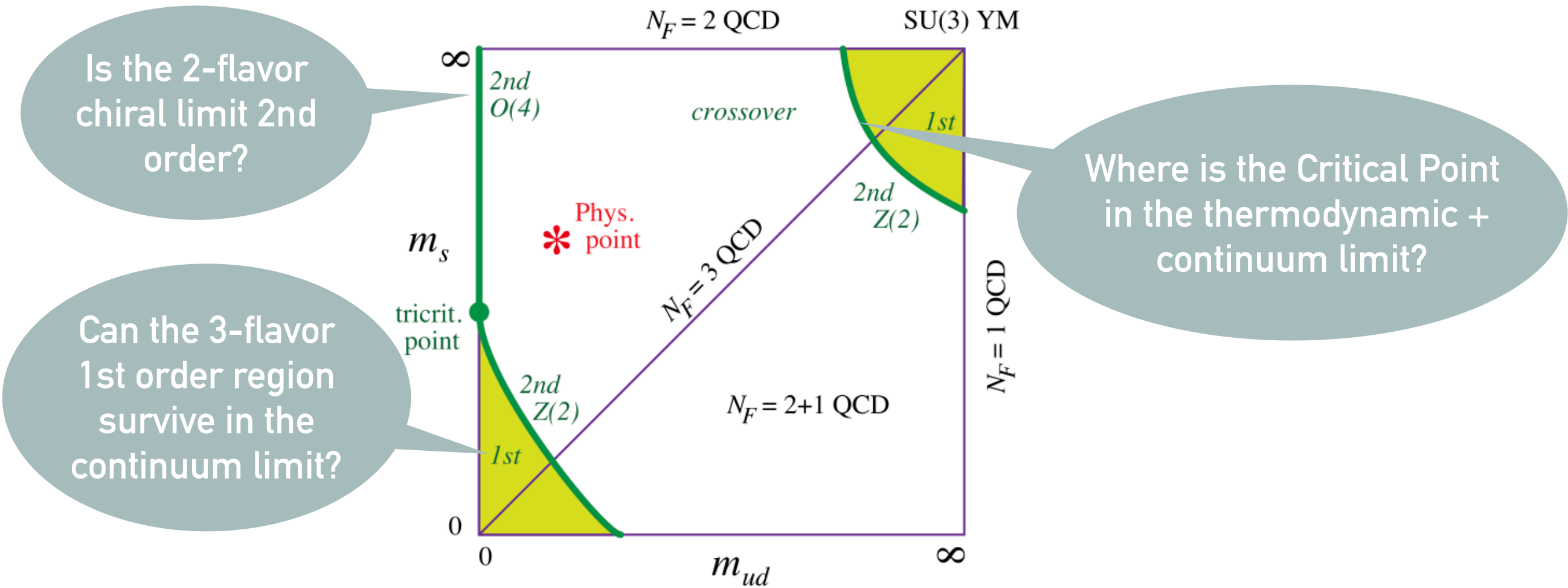
Nature of $T > 0$ QCD transition as function of m_q 's

The traditional picture given by this Columbia plot



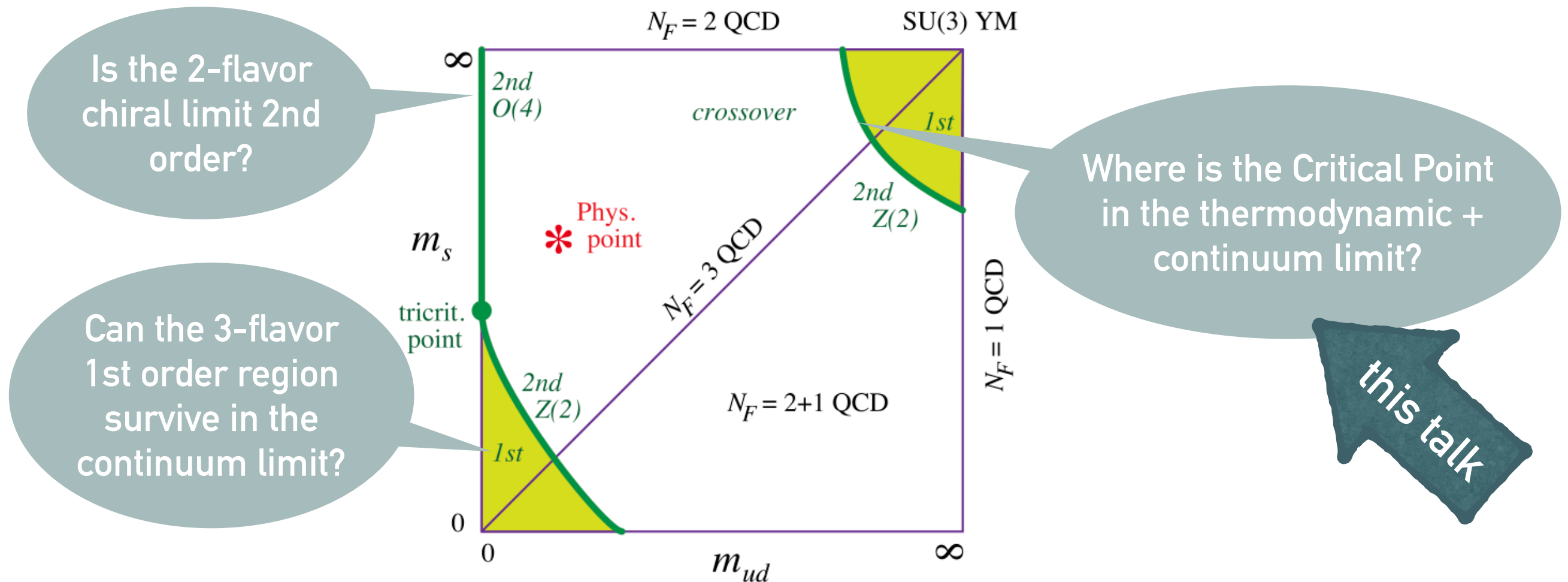
Nature of $T > 0$ QCD transition as function of m_q 's

The traditional picture given by this Columbia plot is still under many discussions...



Nature of $T > 0$ QCD transition as function of m_q 's

The traditional picture given by this Columbia plot is still under many discussions...



Recent studies on the location of CP in heavy-quark QCD

- Saito+ (WQHOT-QCD), *PRD* (2011/2014): HPE LO, $N_t=4$, $N_s/N_t=6$
- Ejiri+ (WHOT-QCD), *PRD* (2020): HPE eff-NLO, $N_t=6$, $N_s/N_t=4-6$; $N_t=8$, $N_s/N_t=3$
- Cuteri+, *PRD* (2021): $N_f=2$, fullQCD, $N_t=6, 8, 10$, $N_s/N_t=4-7(10)$

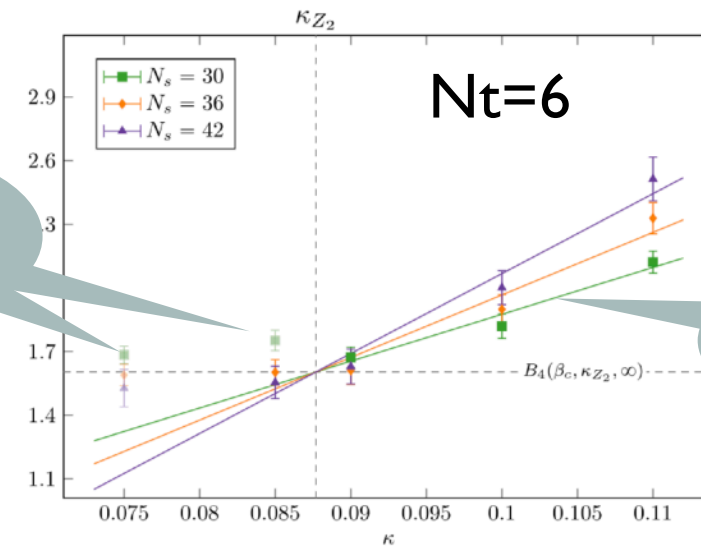
=> We still have strong cutoff & spatial volume dependences.

Motivations

► Binder cumulant analysis based on the $Z(2)$ FSS expected around CP

So far, however, identification of the $Z(2)$ FSS is not a simple task
--- removal of many high-T data required / correction terms to the FSS introduced.

removed



Z(2) FSS fit

(a) Fit e.6.1 at $N_\tau = 6$.

Cuteri+, PRD (2021)

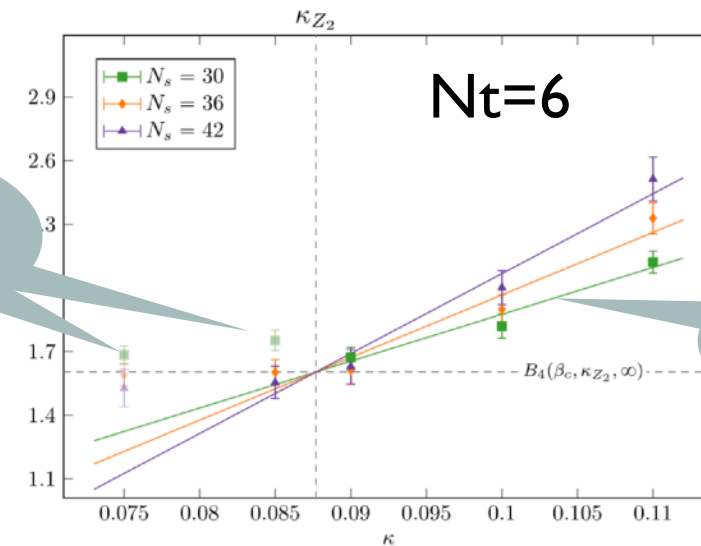
These make the analyses slightly ambiguous & call careful systematic error estimations.

Motivations

► Binder cumulant analysis based on the $Z(2)$ FSS expected around CP

So far, however, identification of the $Z(2)$ FSS is not a simple task
--- removal of many high-T data required / correction terms to the FSS introduced.

removed



$Z(2)$ FSS fit

(a) Fit e.6.1 at $N_\tau = 6$.

Cuteri+, *PRD* (2021)

These make the analyses slightly ambiguous & call careful systematic error estimations.

- => Simulations with larger spatial volumes & high statistics to identify the FSS more clearly.
- => Multi-point reweighting to vary coupling parameters continuously.

This talk is based on

- 🌐 Kiyohara+ (WQHOT-QCD), *Phys.Rev.D* (2021) [DOI: 10.1103/PhysRevD.104.114509]
- 🌐 Wakabayashi+ (WHOT-QCD), *Prog.Theor.Exp.Phys.* (2022) [DOI: 10.1093/ptep/ptac019]
- 🌐 Ashikawa+ (WHOT-QCD), *ongoing*

We first revisit the $N_t=4$ case to increase the spatial volume [Kiyohara+, *PRD* ('21)].

Lattice setup

▶ Action: plaquette gauge + standard Wilson quarks

▶ Kernel for each flavor: $M_{xy}(\kappa) = \delta_{xy} - \kappa \sum_{\mu} \left[(1 - \gamma_{\mu}) U_{x,\mu} \delta_{y,x+\hat{\mu}} + (1 + \gamma_{\mu}) U_{y,\mu}^{\dagger} \delta_{y,x-\hat{\mu}} \right]$
 $= \delta_{xy} - \kappa B_{xy}$ hopping term $\kappa = \frac{1}{2am_q + 8}$

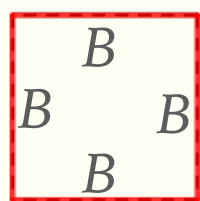
▶ Quark contribution to the effective action: $\ln \det M(\kappa) = -\frac{1}{N_{\text{site}} n} \sum_{n=1}^{\infty} \text{Tr}[B^n] \kappa^n$

● closed loops of B with κ [loop length]

▶ **Hopping Parameter Expansion** to reduce simulation cost for large spatial volumes

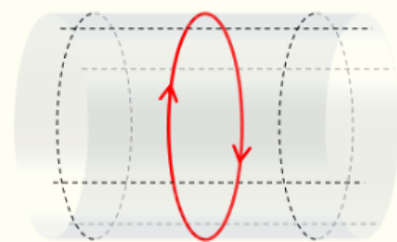
LO:

plaquette



κ^4

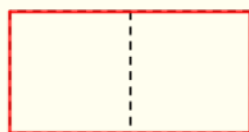
Polyakov loop Ω



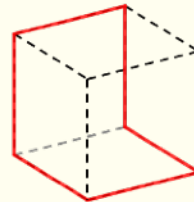
κ^{N_t}

NLO:

(a) rectangle

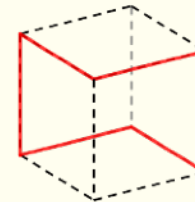


(b) chair

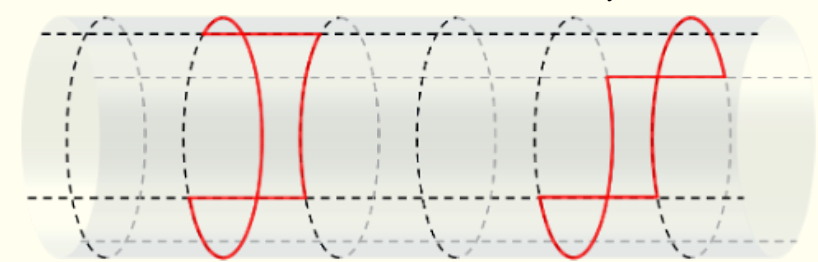


κ^6

(c) crown



bent Polyakov loops Ω_i



κ^{N_t+2}

● HPE $\approx 1/(am_q)$ expansion

● HPE worsens with $a \rightarrow 0$ ($N_t \rightarrow \infty$) \Rightarrow higher order terms required with $N_t \rightarrow \infty$.

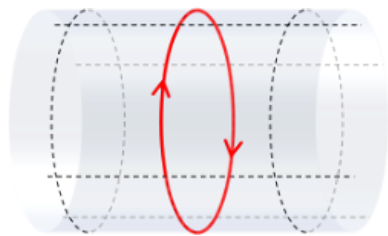
Simulation incorporating LO + NLO meas.'s

Kiyohara, Kitazawa, Ejiri, KK (WHOT-QCD), PRD 104 (2021)

- LO incorporated in the configuration generation



$$\beta \rightarrow \beta^* = \beta + 48N_f\kappa^4$$



$$\lambda \sum_{\mathbf{x}} \Omega(\mathbf{x}) \text{ term in the effective action} \quad (\lambda = 48N_fN_t\kappa^4 \text{ for } N_t=4)$$

can be incorporated in PHB+OR parallel simulation efficiently by keeping all temporal sites within a node

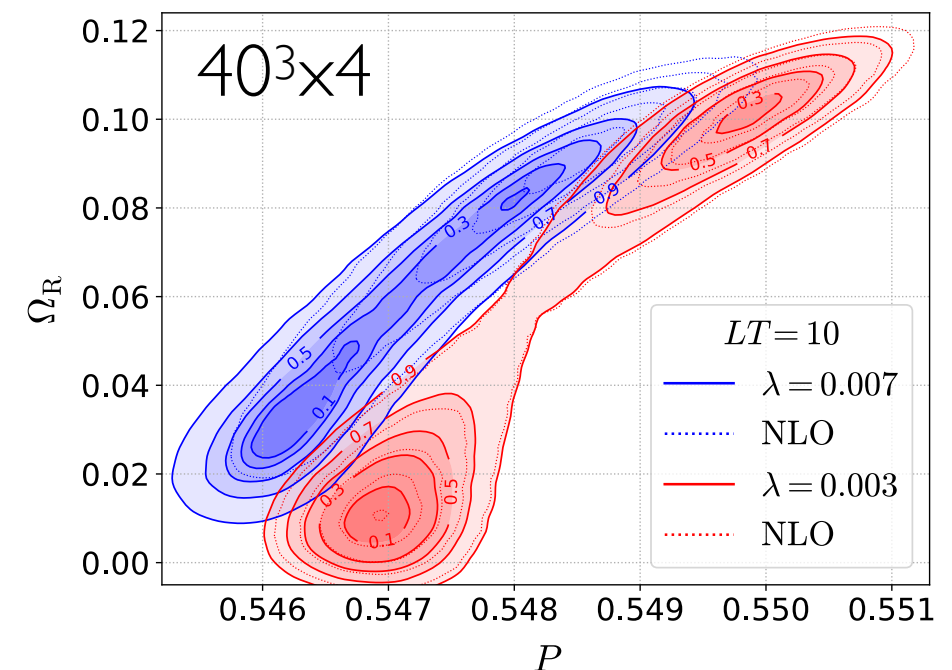
- NLO incorporated in the measurements through multi-point reweighting

$$\langle \hat{O}(U) \rangle_{\beta, \lambda}^{\text{NLO}} = \frac{\langle \hat{O}(U) e^{-\delta S_{\text{LO}} - S_{\text{NLO}}(\beta, \lambda)} \rangle_{\tilde{\beta}, \tilde{\lambda}}^{\text{LO}}}{\langle e^{-\delta S_{\text{g+LO}} - S_{\text{NLO}}(\beta, \lambda)} \rangle_{\tilde{\beta}, \tilde{\lambda}}^{\text{LO}}}$$

$$\delta S_{\text{g+LO}} = S_{\text{g+LO}}(\beta, \lambda) - S_{\text{g+LO}}(\tilde{\beta}, \tilde{\lambda})$$

- Simulations at several $(\tilde{\beta}^*, \tilde{\lambda}) \Rightarrow$ measure at (β^*, λ)

- Overlap problem resolved by the inclusion of LO in configuration generations \Leftarrow essential on spatially large lattices in this study

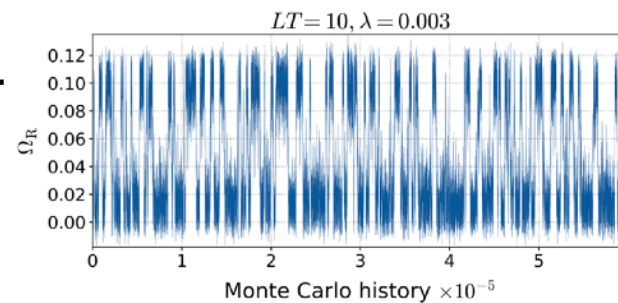


Study on $N_t = 4$ lattices

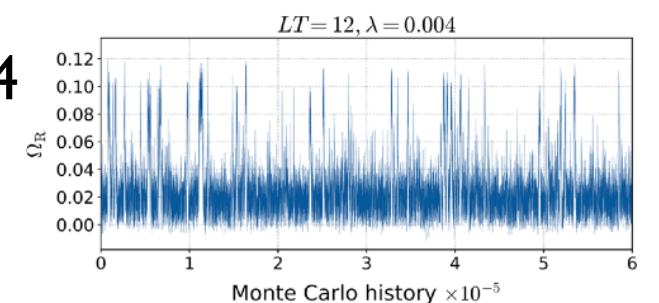
Kiyohara, Kitazawa, Ejiri, KK (WHOT-QCD), *PRD* 104 (2021)

- ▶ Simulations: $N_t=4$, $N_s/N_t = LT = 6, 8, 9, 10, 12$, each $3-6 \times [(\tilde{\beta}^*, \tilde{\lambda})$ with $\sim 10^6$ meas.] around the transition line
 $L = \text{spatial lattice size}$, $\lambda = 48N_f N_t \kappa^4$ for $N_t=4$

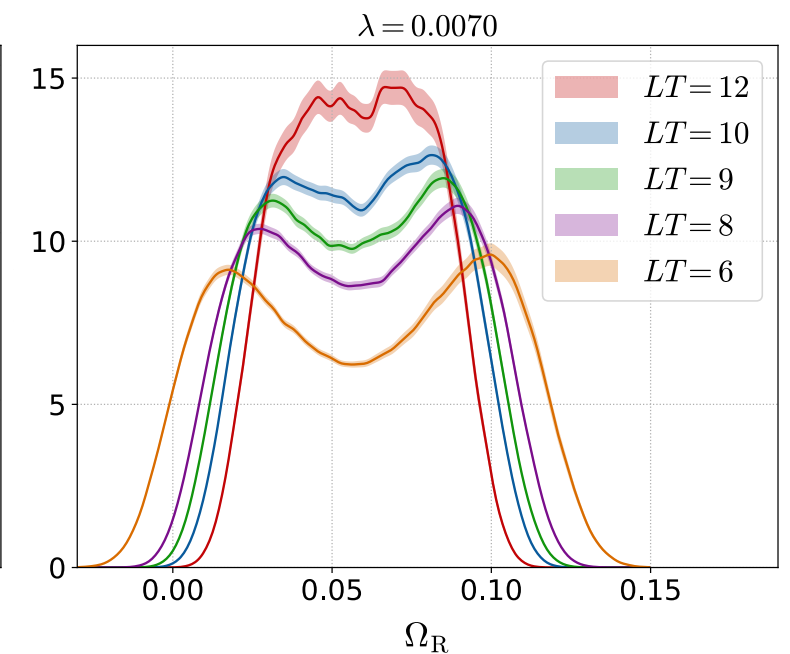
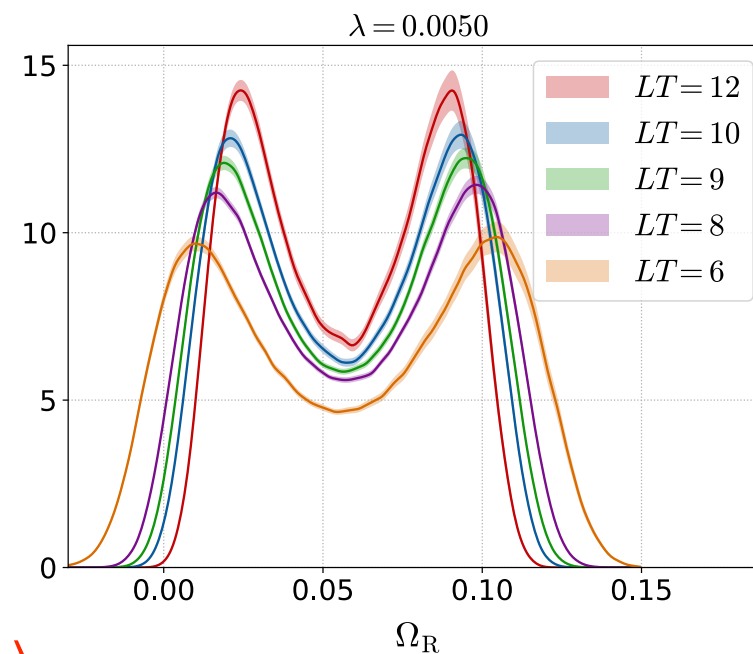
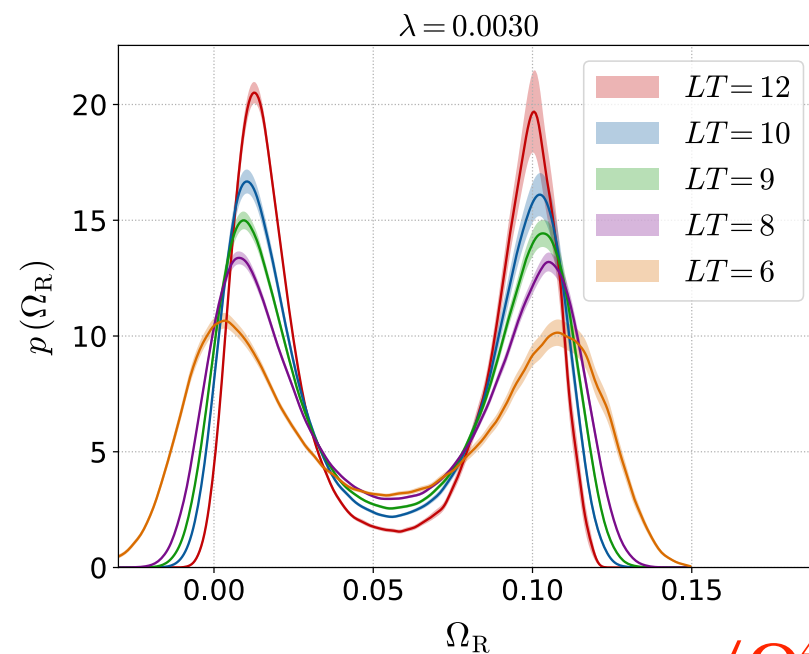
- ▶ History of $\Omega_R = \text{Re}\Omega$ $40^3 \times 4$



$48^3 \times 4$



- ▶ Distribution of Ω_R on the transition line

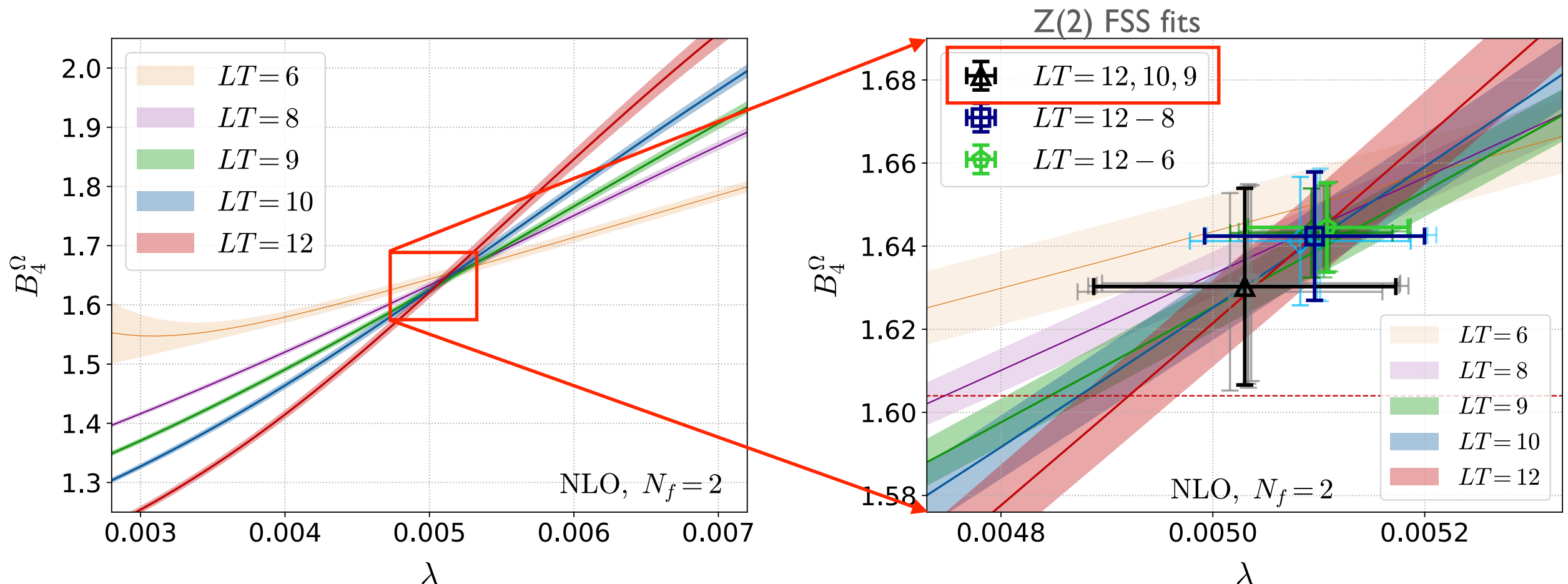


\Rightarrow Binder cumulant $B_4^\Omega = \frac{\langle \Omega_R^4 \rangle_c}{\langle \Omega_R^2 \rangle_c^2} + 3$ along the transition line

Study on $N_t = 4$ lattices

Kiyohara, Kitazawa, Ejiri, KK (WHOT-QCD), *PRD* 104 (2021)

Results at $N_t=4$ with HPE up to NLO



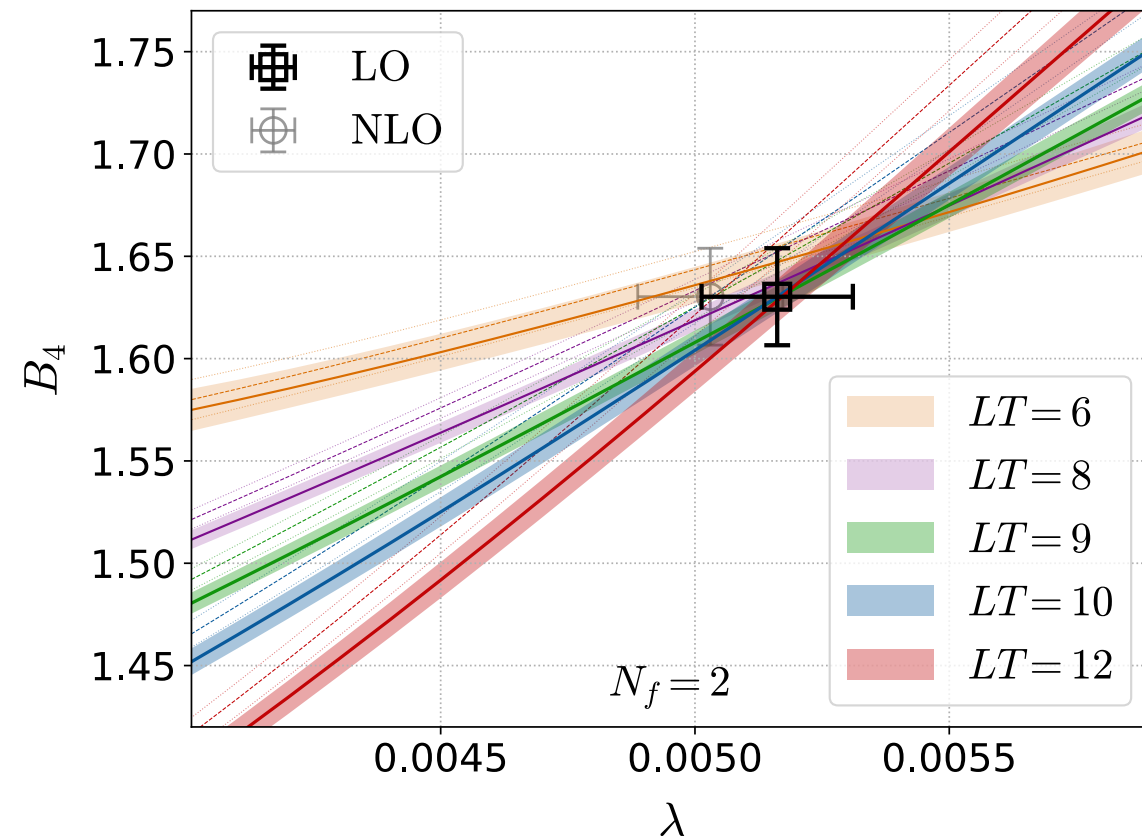
- ★ Precision much improved over previous studies
- ★ $N_s/N_t = LT \geq 9$ required for Z(2) FSS
- ★ $B_4^\Omega = 1.630(24)(2)$ using $N_s/N_t \geq 9$, consistent with Z(2) value 1.604 within $\approx 1\sigma$
- ★ $\lambda_c = 0.00503(14)(2)$ [$\kappa_c = 0.0603(4)$] for $N_t=4, N_f=2$

(cf.) Ejiri+ *PRD*(2020): $\kappa_c = 0.0640(10)$ with eff. NLO

Study on $N_t = 4$ lattices

Kiyohara, Kitazawa, Ejiri, KK (WHOT-QCD), *PRD* 104 (2021)

► Comparison with LO analysis => effects of NLO corrections



★ LO \approx NLO with $N_s/N_t=LT \geq 9$

★ Shift due to NLO is small ($\approx 2.6\%$), suggesting LO dominance around κ_c for $N_t=4$
=> previous $N_t=4$ LO results seems OK

Scope and convergence of HPE

.....
Wakabayashi, Ejiri, KK, Kitazawa (WHOT-QCD), *PTEP* (2022)

Are the effects of further higher orders of HPE really negligible?

Scope and convergence of HPE

Wakabayashi, Ejiri, KK, Kitazawa (WHOT-QCD), PTEP (2022)

Are the effects of further higher orders of HPE really negligible?

► Quark contribution to the effective action:

loops of length n

noise average

$$\ln \det M(\kappa) = N_{\text{site}} \sum_n D_n \kappa^n, \quad D_n = \frac{-1}{N_{\text{site}}^n} \text{Tr}[B^n] \approx \frac{-1}{N_{\text{site}}^n} \langle \langle \eta^\dagger B^n \eta \rangle \rangle_{\text{noises}}$$

$$B_{xy} = \sum_\mu \left[(1 - \gamma_\mu) U_{x,\mu} \delta_{y,x+\hat{\mu}} + (1 + \gamma_\mu) U_{y,\mu}^\dagger \delta_{y,x-\hat{\mu}} \right]$$

Wilson-type loops

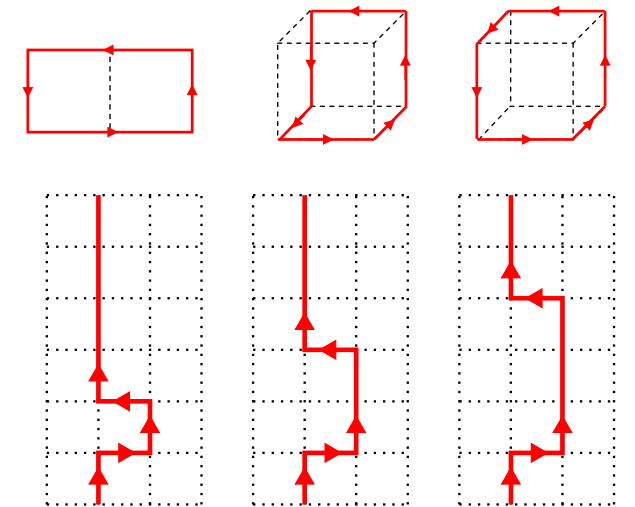
$$W(4) = 96N_c \hat{P}, \quad W(6) = 256N_c (3\hat{W}_{\text{rec}} + 6\hat{W}_{\text{chair}} + 2\hat{W}_{\text{crown}})$$

$$D_n = W(n) + \sum_m L_m(N_t, n) = W(n) + L(N_t, n)$$

Polyakov-type loops with m-windings

$$L_1(N_t, N_t) = \frac{4N_c 2^{N_t}}{N_t} \text{Re} \hat{\Omega}$$

$$L_1(N_t, N_t + 2) = 12N_c 2^{N_t} \sum_k \text{Re} \hat{\Omega}_k$$



We developed a method to separately evaluate $W(n)$ and $L_m(N_t, n)$ from D_n by combing the results with various twisted boundary conditions.

Scope and convergence of HPE

Wakabayashi, Ejiri, KK, Kitazawa (WHOT-QCD), *PTEP* (2022)

- ▶ \hat{W}_i, \hat{P}_j in $W(n)$ and $L_m(N_t, n)$ take their maximum value 1 when we set $U_{x,\mu} = 1$
In this case, we can calculate $W(n)$ and $L_m(N_t, n)$ analytically up to high orders.
=> **Worst convergent case of HPE can be studied by combining them.**

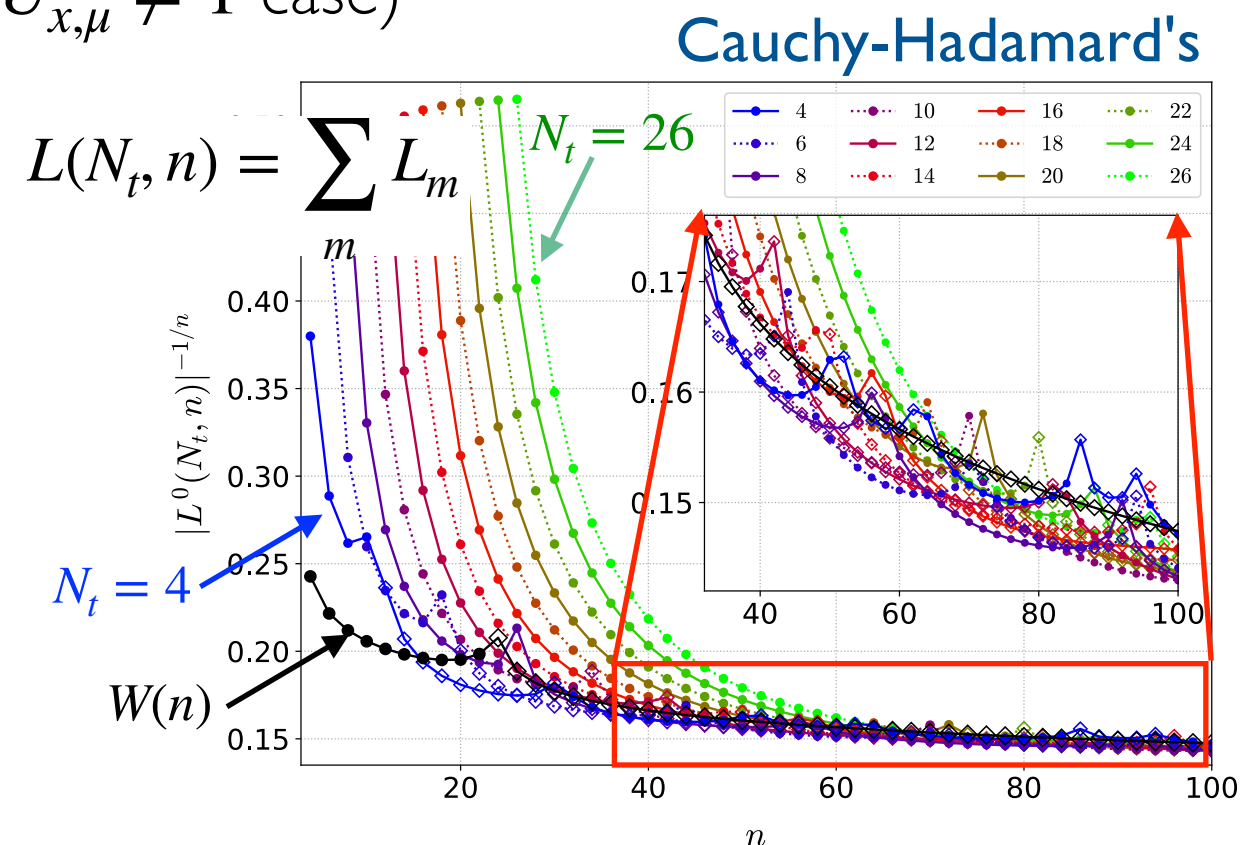
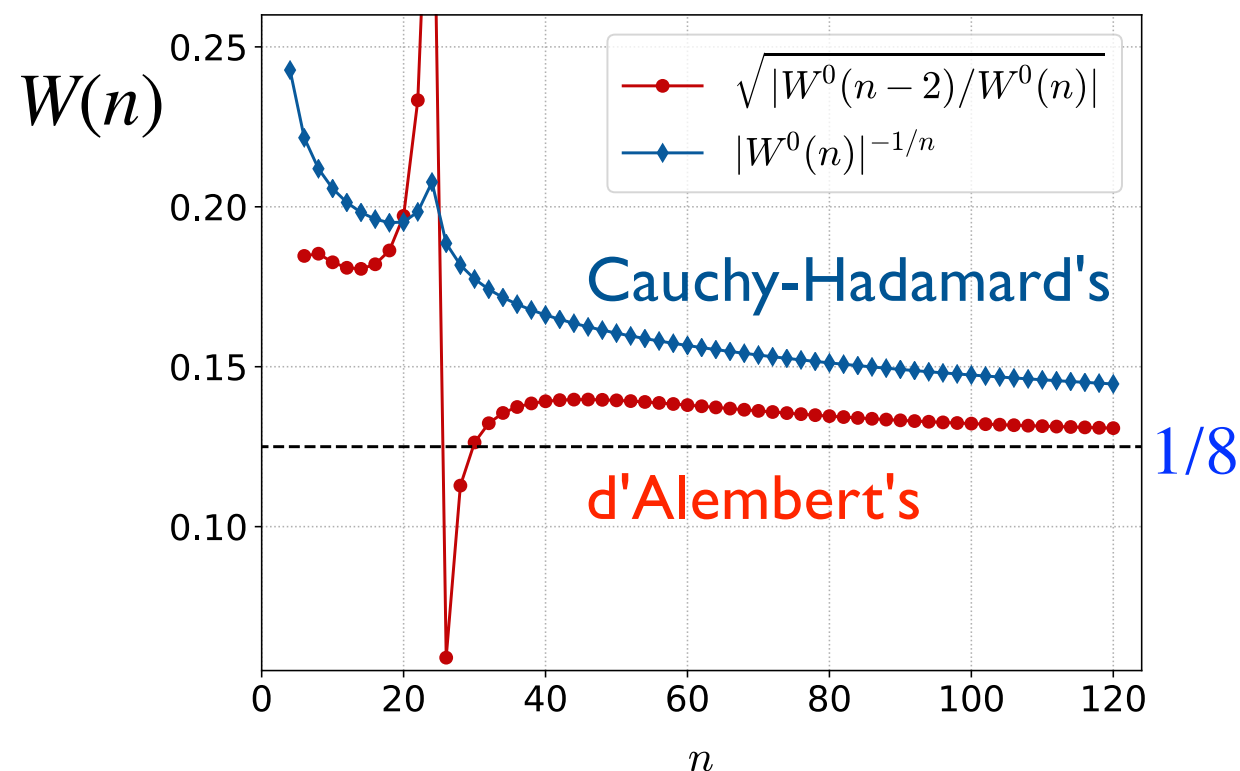
Scope and convergence of HPE

Wakabayashi, Ejiri, KK, Kitazawa (WHOT-QCD), *PTEP* (2022)

- ▶ \hat{W}_i, \hat{P}_j in $W(n)$ and $L_m(N_t, n)$ take their maximum value 1 when we set $U_{x,\mu} = 1$
In this case, we can calculate $W(n)$ and $L_m(N_t, n)$ analytically up to high orders.

=> **Worst convergent case of HPE can be studied by combining them.**

- ◆ **Convergence radius** (lower bound for the $U_{x,\mu} \neq 1$ case)



- ★ Convergence radius $\xrightarrow[n \rightarrow \infty]{} 1/8$, i.e. convergent up to the chiral limit.

<= free Wilson quarks when $U_{x,\mu} = 1$

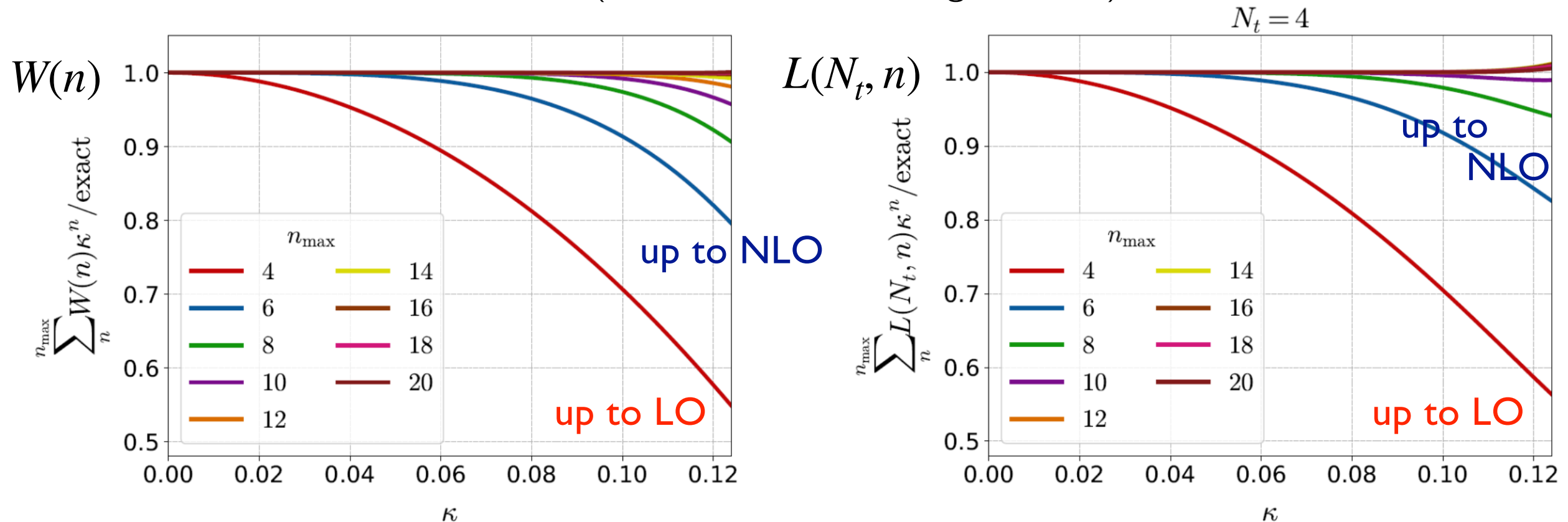
=> **HPE reliable up to the chiral limit when sufficiently high orders are taken.**

Scope and convergence of HPE

Wakabayashi, Ejiri, KK, Kitazawa (WHOT-QCD), *PTEP* (2022)

To which order we need to incorporate? \leq depends on the value of κ

◆ Deviation due to truncation (in the worst convergent case):



★ For $N_t=4$: $\kappa_c = 0.0603(4)$ [Kiyohara+ ('21)]

\Rightarrow LO may have at worst $\approx 10\%$ error, NLO good enough

★ For $N_t=6$: $\kappa_c = 0.0877(9)$ [Cuteri+ ('22)], $0.1286(40)$ [Ejiri+ ('20) using eff. pot.]

\Rightarrow NLO is $\geq 93\%$ accurate. remaining error can be removed by NNLO or higher

★ For $N_t=8$: $\kappa_c = 0.1135(8)$ [Cuteri+ ('22)]

\Rightarrow NNLO needed for $\geq 95\%$ accuracy

Effective method to incorporate high orders

Wakabayashi, Ejiri, KK, Kitazawa (WHOT-QCD), *PTEP* (2022)

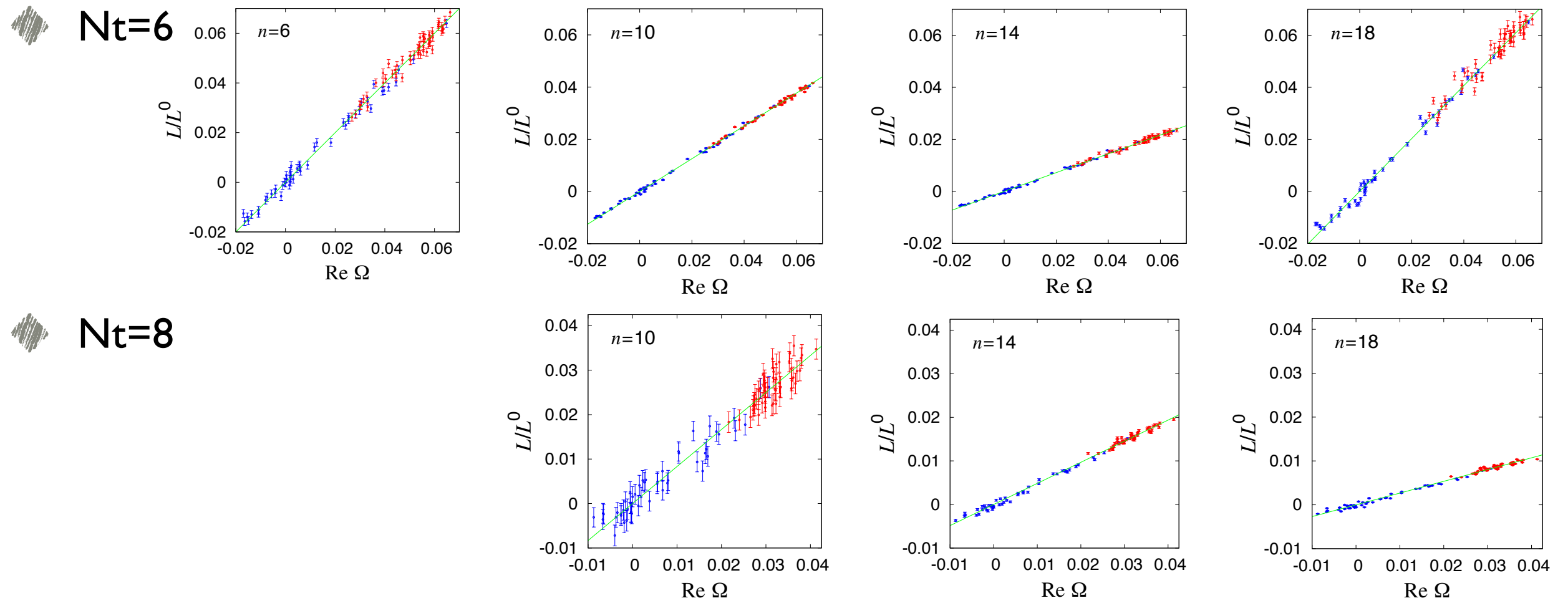
Calculation of high order term becomes quickly difficult with increasing n .

We extend the idea of the effective NLO method [Ejiri+ ('20)] to high orders.

Basic observation: **strong correlation of Wilson/Polyakov-type loops among different n .**

► Distribution of $L(N_t, n)$ vs. the Polyakov loop Ω

- qQCD simulation on $32^3 \times (6, 8)$, blue/red slightly below/above β_{trans}
- normalized by the $U \times \mu = 1$ result L^0



Effective method to incorporate high orders

Wakabayashi, Ejiri, KK, Kitazawa (WHOT-QCD), *PTEP* (2022)

This linear correlation suggests us to approximate

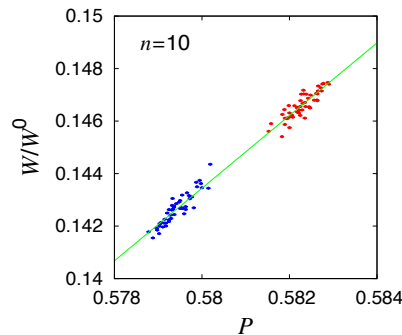
★ $L(N_t, n) \approx L^0(N_t, n) c_n \text{Re}\hat{\Omega}$

known from $U_{x\mu}=1$

our MC results:

	$N_t = 6$	$N_t = 8$
c_6	1	
c_8	0.8112(20)(7)	1
c_{10}	0.6280(15)(3)	0.8327(114)(95)
c_{12}	0.4736(29)(15)	0.6408(36)(27)
c_{14}	0.3609(26)(11)	0.4841(22)(10)
c_{16}	0.3106(25)(10)	0.3616(21)(6)
c_{18}	1.0159(90)(33)	0.2679(16)(3)
c_{20}	-0.02771(57)(13)	0.2020(13)(2)

★ $W(n) \approx W^0(n) (d_n \hat{P} + f_n)$



though the correlation weaker than $L(N_t, n)$

n	$d_n(N_t = 6)$	$f_n(N_t = 6)$	$d_n(N_t = 8)$	$f_n(N_t = 8)$
4	1	0	1	0
6	1.3625(73)(12)	-0.4070(42)(7)	1.3366(66)(8)	-0.3922(39)(5)
8	1.4644(123)(11)	-0.6089(72)(6)	1.4256(96)(8)	-0.5869(57)(5)
10	1.3835(156)(10)	-0.6590(91)(6)	1.3433(117)(8)	-0.6367(70)(5)
12	1.2140(178)(9)	-0.6235(103)(5)	1.1752(130)(7)	-0.6025(78)(4)
14	1.0256(196)(9)	-0.5533(114)(5)	0.9825(141)(7)	-0.5303(85)(4)
16	0.8607(219)(9)	-0.4811(127)(5)	0.8052(153)(8)	-0.4512(92)(5)
18	0.7481(258)(10)	-0.4296(150)(6)	0.6698(173)(9)	-0.3870(103)(5)
20	0.7290(337)(12)	-0.4275(196)(7)	0.6071(219)(12)	-0.3606(131)(7)

=> Higher order effects can be effectively incorporated in the LO simulation by

$$\beta \rightarrow \beta^* = \beta + \frac{1}{6} N_f \sum_{n=4}^{n_{\max}} W^0(n) d_n \kappa^n \quad \lambda \rightarrow \lambda^* = N_f N_t \sum_{n=N_t}^{n_{\max}} L^0(N_t, n) c_n \kappa^n$$

Extension to non-degenerate cases ($N_f=2+1$ etc.) straightforward.

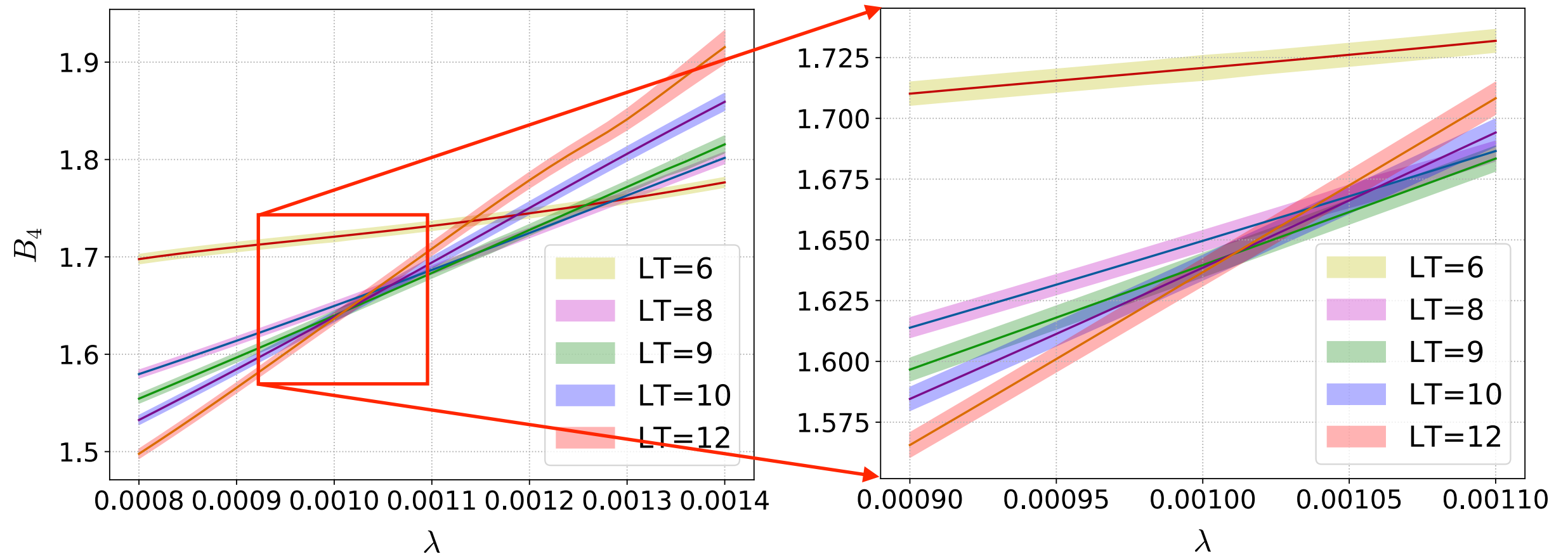
Study on $N_t = 6$ lattices

Ashikawa+ (WHOT-QCD), *ongoing*

▶ $N_t=6$, $N_s/N_t = LT = 6, (7,) 8, 9, 10, 12, (15)$ *ongoing*

▶ Status of B_4^Ω with NLO:

$\lambda = 128N_f N_t \kappa^6$ for $N_t=6, N_f=2, \text{NLO}$



Preliminary:

★ $B_4^\Omega \sim 1.63 - 1.64$ with $N_s/N_t \geq 9$ (cf.) $Z(2)$ value = 1.604

★ $\lambda_c \sim 0.00101 \Rightarrow \kappa_c \sim 0.093$ NLO $\Rightarrow \kappa_c \sim 0.0905$ eff. including up to 20th order
looks consistent with $\kappa_c = 0.0877(9)$ by a full QCD simulation [Cuteri+ ('22)]

Conclusion & outlook

★ **HPE provides us with a reliable and powerful way to study QCD with heavy quarks**

- ☑ Convergent up to chiral limit + enable large N_s/N_t simul.'s + analytic in N_f
- ☑ up to κ_c of $N_t=4, N_f=2$: LO: $\geq 90\%$ / NLO: $\geq 99\%$ accurate
- ☑ around κ_c of $N_t=6, N_f=2$: NLO: $\geq 93\%$ accurate

Higher orders needed to remove remaining truncation error and for $N_t \geq 8$.

★ **At $N_t=4$, $N_s/N_t \geq 9$ needed for $Z(2)$ FSS**

=> NLO study of B_4^Ω : $\kappa_c = 0.0603(4)$ for $N_f=2$

★ At $N_t=6$ with $N_s/N_t \geq 9$, $\kappa_c \sim 0.090$ including high orders (preliminary) looks consistent with a full QCD study [Cuteri+ ('22)]

🌀 At $N_t=6$, more statistics & larger N_s/N_t : ongoing

🌀 Continuum extrapolation => large N_t => high orders must be taken.

★ **We developed an effective method to incorporate high orders**

=> easy to implement in LO PHB simulations => used in $N_t=6$ study

🌀 HPE powerful also at **finite densities** : in progress (cf.) Chabane on Monday

We miss our best friend+collaborator

Yusuke Taniguchi

who passed away silently on July 22, 2022.



1968-2022

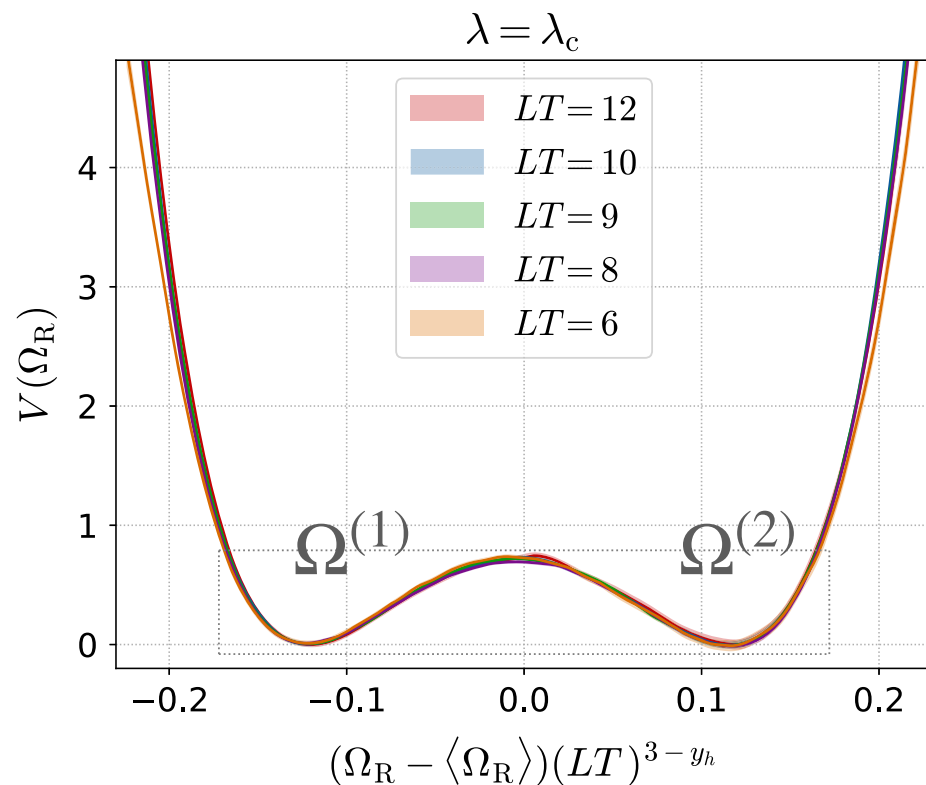
backup slides



backup slides

Kiyohara, Kitazawa, Ejiri, KK (WHOT-QCD), *PRD* 104 (2021)

$$V(\Omega_R; \lambda, LT) = -\ln p(\Omega_R)_{\lambda, LT},$$



$$\Delta\Omega = \Omega^{(2)} - \Omega^{(1)}. \quad (46)$$

According to Eq. (15), this quantity should behave around the *CP* as

$$\Delta\Omega(\lambda, LT) = (LT)^{y_h-3} \Delta\tilde{\Omega}((\lambda - \lambda_c)(LT)^{1/\nu}), \quad (47)$$

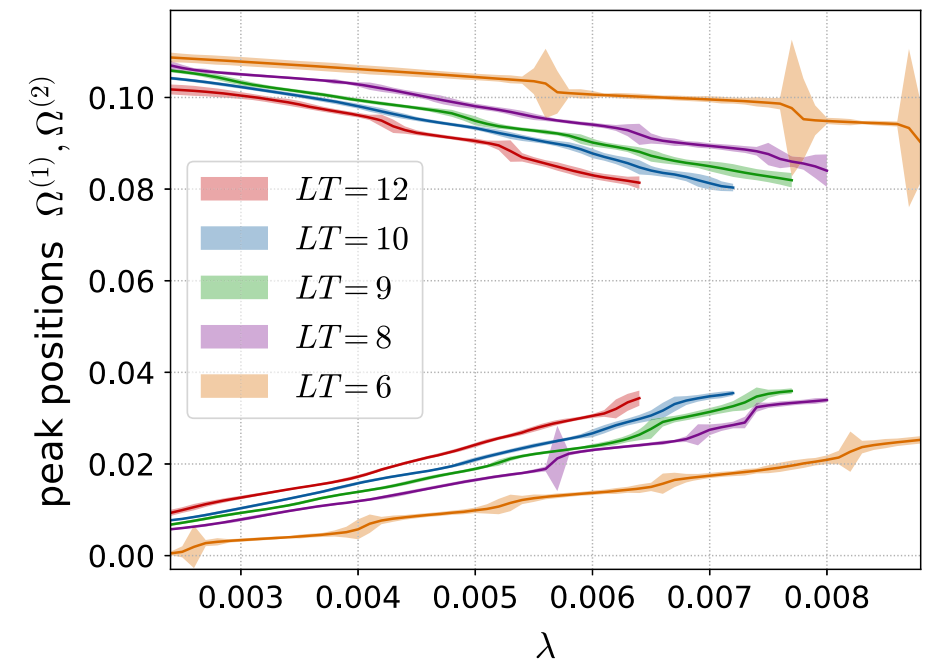
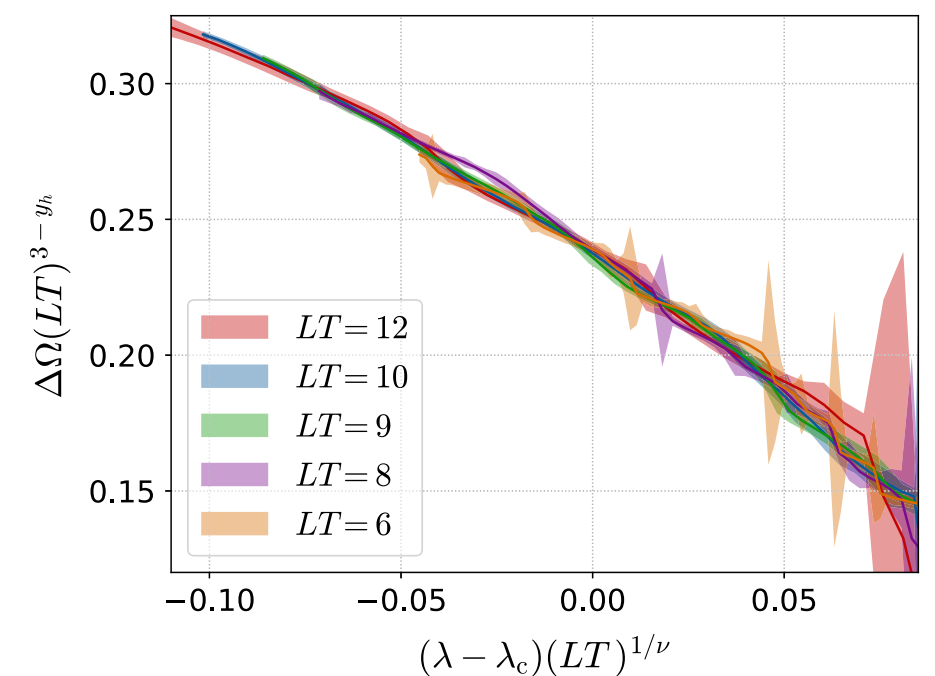


FIG. 13. Positions of peaks of the distribution function $p(\Omega_R)$ measured on the transition line.



backup slides

Wakabayashi, Ejiri, KK, Kitazawa (WHOT-QCD), PTEP (2022)

$W^0(4)$	288	$W^0(20)$	$1.54422361 \times 10^{14}$	$W^0(36)$	$-5.58410362 \times 10^{27}$
$W^0(6)$	8448	$W^0(22)$	$2.83682900 \times 10^{15}$	$W^0(38)$	$-2.91018925 \times 10^{29}$
$W^0(8)$	245952	$W^0(24)$	$-2.40028584 \times 10^{16}$	$W^0(40)$	$-1.50223497 \times 10^{31}$
$W^0(10)$	7372800	$W^0(26)$	$-6.88836562 \times 10^{18}$	$W^0(42)$	$-7.71380102 \times 10^{32}$
$W^0(12)$	225232896	$W^0(28)$	$-5.41133954 \times 10^{20}$	$W^0(44)$	$-3.95168998 \times 10^{34}$
$W^0(14)$	6906175488	$W^0(30)$	$-3.39122203 \times 10^{22}$	$W^0(46)$	$-2.02386871 \times 10^{36}$
$W^0(16)$	208431502848	$W^0(32)$	$-1.93668514 \times 10^{24}$	$W^0(48)$	$-1.03783044 \times 10^{38}$
$W^0(18)$	$6.00259179 \times 10^{12}$	$W^0(34)$	$-1.05424635 \times 10^{26}$	$W^0(50)$	$-5.33468075 \times 10^{39}$

$L_1^0(4, 4)$	48	$L_1^0(10, 10)$	1228.8	$L_1^0(18, 18)$	174762.67
$L_1^0(4, 6)$	1728	$L_1^0(10, 12)$	331776	$L_1^0(18, 20)$	160432128
$L_1^0(4, 8)$	45792	$L_1^0(10, 14)$	52862976	$L_1^0(18, 22)$	75497472000
$L_1^0(4, 10)$	645120	$L_1^0(10, 16)$	6258180096	$L_1^0(18, 24)$	2.36626×10^{13}
$L_1^0(4, 12)$	-26224128	$L_1^0(10, 18)$	5.99330×10^{11}	$L_1^0(18, 26)$	5.50232×10^{15}
$L_1^0(4, 14)$	-3201067008	$L_1^0(10, 20)$	4.87727×10^{13}	$L_1^0(18, 28)$	1.01809×10^{18}
$L_1^0(4, 16)$	-2.14087×10^{11}	$L_1^0(10, 22)$	3.47446×10^{15}	$L_1^0(18, 30)$	1.57315×10^{20}
$L_1^0(4, 18)$	-1.19007×10^{13}	$L_1^0(10, 24)$	2.20156×10^{17}	$L_1^0(20, 20)$	629145.6
$L_1^0(4, 20)$	-6.00757×10^{14}	$L_1^0(10, 26)$	1.24531×10^{19}	$L_1^0(20, 22)$	717225984
$L_1^0(4, 22)$	-2.84486×10^{16}	$L_1^0(10, 28)$	6.20798×10^{20}	$L_1^0(20, 24)$	4.11140×10^{11}
$L_1^0(4, 24)$	-1.28105×10^{18}	$L_1^0(10, 30)$	2.59861×10^{22}	$L_1^0(20, 26)$	1.54445×10^{14}
$L_1^0(4, 26)$	-5.50874×10^{19}	$L_1^0(12, 12)$	4096	$L_1^0(20, 28)$	4.24543×10^{16}
$L_1^0(4, 28)$	-2.25576×10^{21}	$L_1^0(12, 14)$	1622016	$L_1^0(20, 30)$	9.17892×10^{18}
$L_1^0(4, 30)$	-8.69402×10^{22}	$L_1^0(12, 16)$	360603648	$L_1^0(22, 22)$	2287802.18
$L_1^0(6, 6)$	128	$L_1^0(12, 18)$	57416810496	$L_1^0(22, 24)$	3170893824
$L_1^0(6, 8)$	11520	$L_1^0(12, 20)$	7.19497×10^{12}	$L_1^0(22, 26)$	2.17478×10^{12}
$L_1^0(6, 10)$	716544	$L_1^0(12, 22)$	7.51820×10^{14}	$L_1^0(22, 28)$	9.64167×10^{14}
$L_1^0(6, 12)$	35891712	$L_1^0(12, 24)$	6.80443×10^{16}	$L_1^0(22, 30)$	3.09123×10^{17}
$L_1^0(6, 14)$	1464910848	$L_1^0(12, 26)$	5.46987×10^{18}	$L_1^0(24, 24)$	8388608
$L_1^0(6, 16)$	43817011200	$L_1^0(12, 28)$	3.96931×10^{20}	$L_1^0(24, 26)$	13891534848
$L_1^0(6, 18)$	3.17933×10^{11}	$L_1^0(12, 30)$	2.62442×10^{22}	$L_1^0(24, 28)$	1.12307×10^{13}
$L_1^0(6, 20)$	8.54676×10^{13}	$L_1^0(14, 14)$	14042.42	$L_1^0(24, 30)$	5.80075×10^{15}

backup slides

Wakabayashi, Ejiri, KK, Kitazawa (WHOT-QCD), *PTEP* (2022)

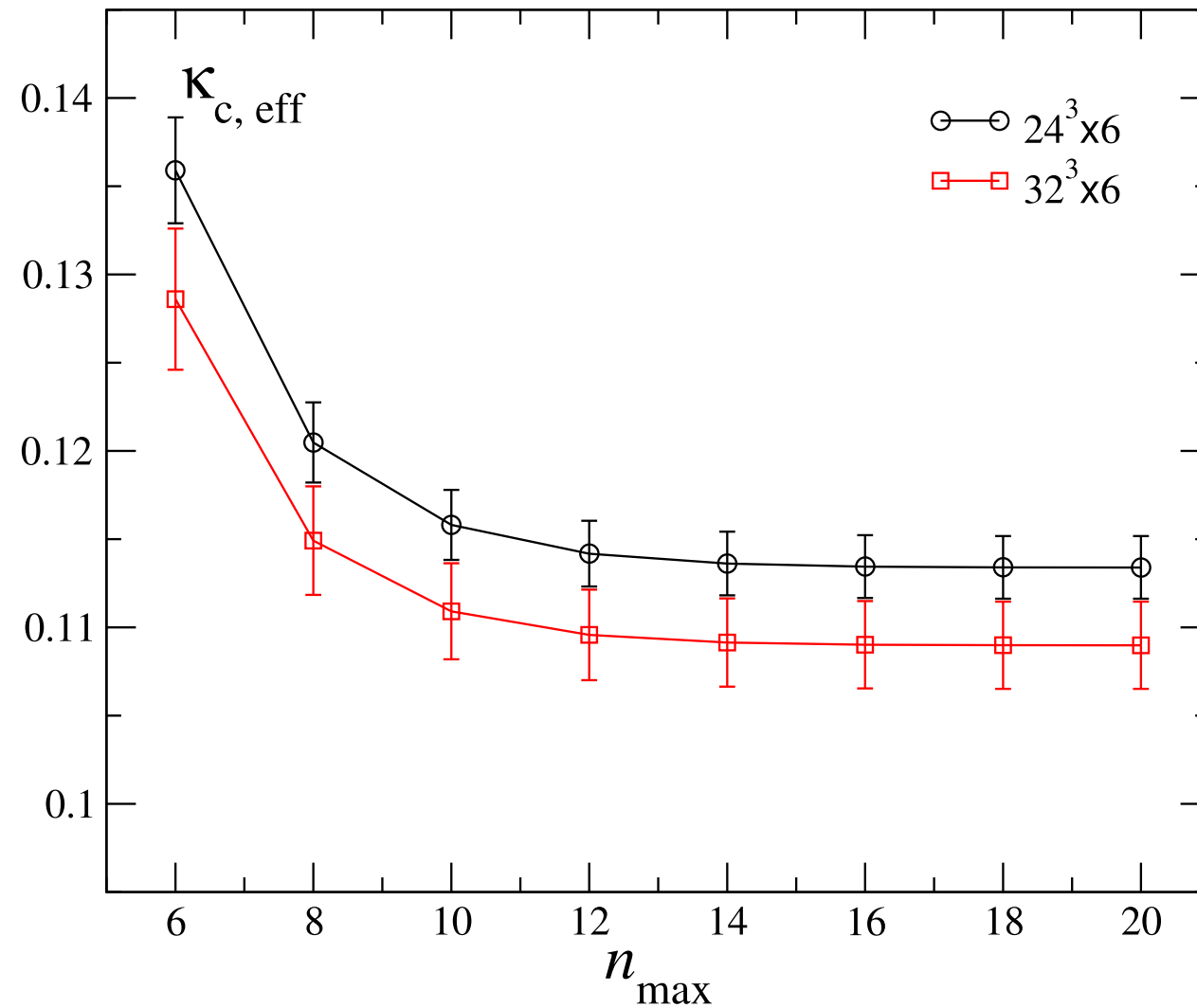


Fig. 11. Effective critical point $\kappa_{c, \text{eff}}$ in two-flavor QCD for $N_t = 6$ as a function of n_{max} . The black circle and red square symbols are for $\kappa_{c, \text{LO}}$ obtained on a $24^3 \times 6$ and a $32^3 \times 6$ lattice, respectively.

backup slides

Wakabayashi, Ejiri, KK, Kitazawa (WHOT-QCD), *PTEP* (2022)

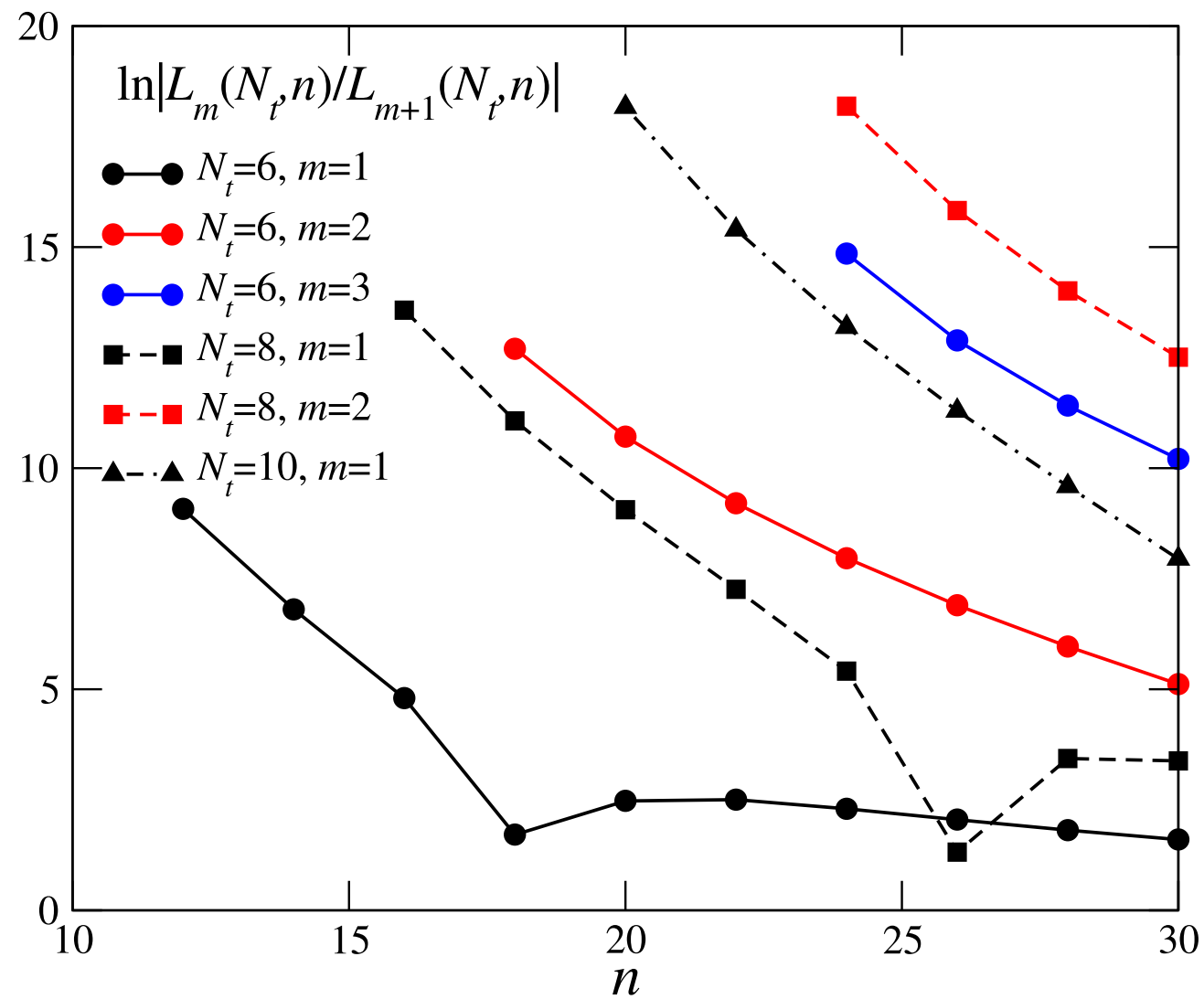


Fig. 14. Upper bound of μ/T such that higher- m terms are small, as given in Eq. (71).

$$\frac{\mu}{T} < \ln \left| \frac{L_m^0(N_t, n)}{L_{m+1}^0(N_t, n)} \right|$$